



Removal of Phenol Contaminants from Aqueous Solution Using Pickering Emulsion Liquid Membrane Stabilized by Magnetic Nano-Fe₃O₄

Tamara L. Rasool ^{a,*}, Ahmed A. Mohammed ^a, Vida Ravankhah ^b

^a Environmental Engineering Department, College of Engineering, University of Baghdad, Baghdad, Iraq

^b Chemical Engineering Department, Kermanshah University of Technology, Kermanshah, Iran

Abstract

In the current study, the effect of the nonionic surfactant (span 80) on the emulsification of a mixture of kerosene as a petroleum-based organic solvent and span80 as a green diluent in the ratio 1:1 was investigated. NaOH was used as the internal phase, and the stability of the emulsion was tested. The potential for extracting phenol from aqueous solutions without the use of a carrier agent has been explored using Pickering emulsion liquid membrane. Additionally, the impacts of experimental parameters include homogenizer speed, mixing speed, emulsification time, Fe₃O₄-Span 80 ratios, NaOH concentration, and internal to membrane volume ratio (I/O) on extraction effectiveness and emulsion stability. The findings demonstrated that after 9 minutes of contact time and a minimum breaking percent of 0.745% under ideal circumstances, more than 96% of phenol could be recovered. In addition thermodynamic analysis reveals that the extraction process was an endothermic and spontaneous in nature and the overall mass transfer coefficient was 1.115×10^{-6} m/s. Membrane materials and nanoparticles were recycled four time in the extraction of phenol with approximately the same efficiency and no significant breakage percent.

Keywords: Pickering emulsion liquid membrane; Stripping; Efficiency; Emulsion stability; Extraction; Breakage.

Received on 07/07/2023, Received in Revised Form on 18/10/2023, Accepted on 18/10/2023, Published on 30/03/2024

<https://doi.org/10.31699/IJCPE.2024.1.15>

1- Introduction

Various industrial and manufacturing processes produce multiple types of wastewater that introduce toxic contaminants into water and groundwater. This causes serious environmental concern, primarily because these industrial waste contaminants are known to be hazardous. Hydrocarbons such as phenolic compounds of 4-Nitrophenol and other derivatives are often found in wastewater of many industrial processes [1]. The capacity of 4-Nitrophenol and other compounds to destroy vital organs like the kidneys, central nervous system, liver, and blood cells in the human and animal body has caused the United States Environmental Protection Agency (USEPA) to classify them as toxic aquatic substances [2]. As a result, before being released into the environment, the wastewater produced by these companies needs to undergo effective treatment. It's possible that phenol cannot be effectively eliminated by conventional treatment of wastewater techniques; In order to remove phenol from wastewaters, a potent Pickering emulsion liquid membrane (PELM) method is being developed.

A modified version of the conventional Emulsion liquid membrane technology is called PELM. When it comes to the removal and recovery of numerous valuable organic and inorganic contaminants from aqueous solutions, ELM, which was first discovered by Norman

[3], is still regarded by many researchers as being more effective than other wastewater treatment techniques like chemical precipitation, ion exchange [4], ozonation and advance oxidation [5], biosorption [6], adsorption [7,8], pressure-driven membrane processes and electrochemical processes [9, 10].

PELM is a three phases dispersion system in general, consisting of two insoluble organic phases (membrane) and two soluble liquid aqueous phases (external and interior). The can considerably improve the membrane phase's reutilization for additional processes of extraction and can lower energy usage. PEs are occasionally brownish or black rather than generally milky white [11, 12], or reddish (brown) [13] depending on the type of nanoparticles used. In this work, the Pickering emulsion was stabilized using magnetic Fe₃O₄ nanoparticles. Previous research have demonstrated that Fe₃O₄ has magnetic properties. [14, 15], These nanoparticles display special nanoscale qualities including being the most stable iron oxide, biocompatible, low toxicity, and ecologically benign [16, 17]. To make a water-in-oil (w/o) Pickering emulsion, the aqueous inner phase and organic oil phase are homogenized with nanoparticles acting as a stabilizing factor. Because of their high stability, nanomaterial-stabilized emulsions have attracted a lot of attention [18,



*Corresponding Author: Email: tamara.Luay2111m@coeng.uobaghdad.edu.iq

© 2024 The Author(s). Published by College of Engineering, University of Baghdad.

This is an Open Access article licensed under a [Creative Commons Attribution 4.0 International License](https://creativecommons.org/licenses/by/4.0/). This permits users to copy, redistribute, remix, transmit and adapt the work provided the original work and source is appropriately cited.

19]. PELM has a number of significant advantages above conventional wastewater treatment techniques, including large removal and recovery efficiency, extraction and stripping in the same period of time system, cheap costs, a low degree of toxicity, a large mass transfer interfacial area, and increased permeate flux [20, 21]. A significant advantage of PELM stabilized by magnetic nano- Fe_3O_4 particles is their greater stability under a variety of experimental conditions. Additionally, after the extraction process, the magnetic can be easily de-emulsified by applying an external magnetic field to quickly attract the particle emulsifier from the emulsion surfaces.

2- Materials and Experimental Methods

2.1. Materials

The laboratory grade reagents used are Crystals of phenol (99.5% assay) obtained from India (ALPHA CHEMIKA), Span 80 as a surfactant, pellets of sodium hydroxide (NaOH, 98% purity), nanoparticle (Fe_3O_4) as a stabilizing agent. The fact that everyone for the use was of analytical quality negated the need for any additional purification. For the preparation of aqueous solutions, water that was distilled was employed.

2.2. Preparation of Pickering emulsion

Certain amounts of Fe_3O_4 and span80 were homogenized after being distributed in 25 milliliters of kerosene with the assistance of an ultrasonication speed homogenizer (SR30). Following the addition of 25 milliliters of a water solution of NaOH in a dropwise fashion, the oil phase was homogenized utilizing a rapid-speed homogenizer (SR30, USA) with a specified emulsification duration. This was done before the homogenization process began.

2.3. Pickering emulsion liquid membrane process

External or feed phase stock solution of 100 ppm phenol solution dissolved in distilled water. A mechanical agitator was used to stir the external phase in the beaker at an appropriate speed, and then the main Pickering emulsion was then added into the external phase while it was constantly agitated at room temperature for a set amount of time shown in Fig. 1 and Table 1. After that, the entire mixture was put into a separator funnel for 9 minutes so that the external phase and the emulsion phase could become distinct from one another. Utilizing a funnel that separates, both the emulsion phase at the top and the aqueous phase at the bottom were separate. After separating the aqueous phase from the upper phase using a magnet, the particles could then be recovered from the water phase using a filter. The collected particulates were then given a final washing in water that had been deionized before being dried using a Hoover oven at 55 degrees Celsius in (10 h). The washed Fe_3O_4 and to create a novel Pickering emulsion, the organic phase was utilized. The concentration of phenol in an aqueous

solution was measured using ultraviolet-visible (UV-Vis) spectrophotometry for 270 nm absorbance at a number of different time intervals.

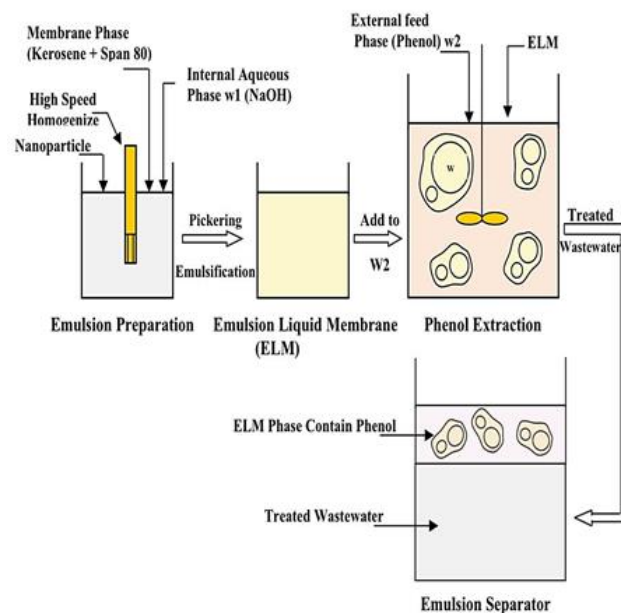


Fig. 1. Shows the Steps of Operating the PELM Process

Table 1. Operating Parameters for PELM System

Ranges	Unit	Parameter
Homogenizer speed	rpm	3000,5800,12700
Emulsion to the external ratio		25:250,50:250,100:250
Fe_3O_4	%(w/v)	0.1,0.2,0.4,0.6
Mixing speed	rpm	200,250,300,350
Internal-to-membrane ratio		10:25,15:25,25:25
Emulsification Time	min	3, 5, 7
Surfactant concentration	%(v/v)	2,4,6,8

3- Analysis and Calculations

A UV spectrophotometer was utilized to determine the phenol concentrations in the external phase. Utilizing the standard method and calibration curve, their concentrations have been calculated.

Once the two-phase emulsion has been removed of emulsion and separated into oil and internal aqueous phases, the peeling process can begin. Eq. 1 can be used to figure out how much phenol has been recovered from its membrane phase.

$$\%S = \frac{C_{if}}{C_{eo} - C_{ef}} * 100 \quad (1)$$

Where C_{if} and C_{ef} are the final concentrations of solute in the internal and external phases, respectively.

The emulsion breakage ($\% \xi$) can be defined as mass balance from the pre- and post-extraction pH of the external solute is used to calculate the volume of the ratio lost during phase external (V_i) for the volume of the internal phase (V_{io}). as described in Eq. 2 and Eq. 3.

$$\% \xi = \frac{V_i}{V_{io}} * 100 \quad (2)$$

$$V_i = V_{\text{ext}} \frac{10^{\text{pH}_0 - 14} - 10^{\text{pH} - 14}}{10^{\text{pH} - 14} - c_{\text{OH}^-}^{\text{int}}} \quad (3)$$

Where V_{ext} : is the volume of the initial external phase. $c_{\text{OH}^-}^{\text{int}}$: is the starting concentration OH^- within the internal phase. pH_0 : is the initial for the feed of phase. pH : was the of the solution for the feed of phase after a specified amount of time has passed.

4- Results and Discussion

4.1. XRD Characterization

Fig. 2 displays the X-ray diffraction pattern produced by magnetite nanoparticles. with crystal planes

corresponding to diffraction peaks [22], with a typical pattern of a spinel inverse structure, signifying the formation of magnetite (Fe_3O_4). $D = 0.92\lambda / (2\theta) \cos \theta$, where D represents crystalline domain size, (λ) resembles x-ray wavelength ($\lambda = 1.5418 \text{ \AA}$), and (2θ) represents full width at half-maximum of the strongest peak.

XRD patterns of the composite showed distinct peaks at 2θ values of 30.1, 35.5, 43.1, 57.1, and 62.6, which correspond to the characteristic peaks of Fe_3O_4 (JCPDS card number 19-0629) [23]. We can observe that the material tends to have fewer disorders or less entropy change than pure Fe_3O_4 due to the re-crystallization of the agglomerated particles.

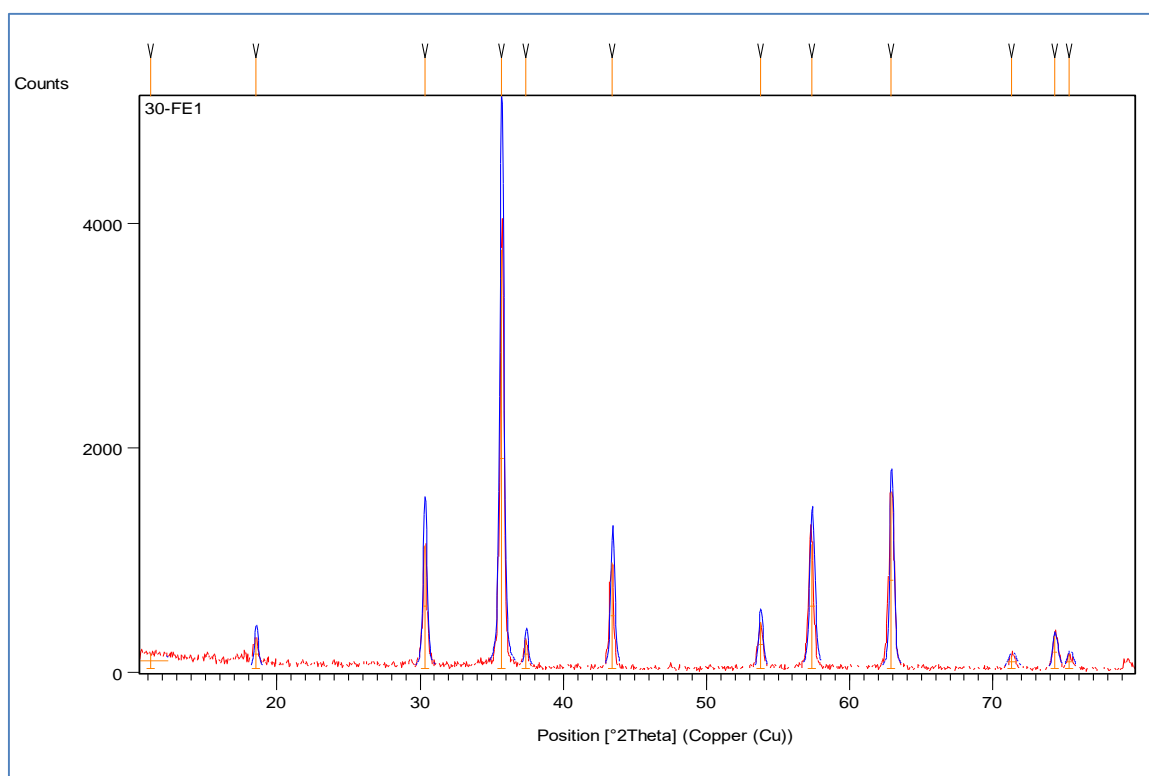


Fig. 2. XRD Diffract Graph for Fe_3O_4 Nanoparticles

4.2. SEM Measurement

The scanning electron microscope (SEM) was utilized to examine the structure features of hematite nanoparticles, including their particle size and morphology. These findings are illustrated in Fig. 3. Observing pure and modified Fe_3O_4 nanoparticles in both figures, pure nanoparticles seem to be aggregated in an irregular shape due to their high surface energy, the nano-size of the Fe_3O_4 , of an average size is about 166 nm. After modification, the size of particles was changed to be around 95 nm, and the nanoparticles have sharper (more defined) agglomeration and narrow size distribution.

4.3. Effect of Homogenizer Speed

It is one of the most essential aspects that has a considerable influence on both the stability of the PELM

and the entire process of extraction the speed at which the homogenizer runs. We tested speeds between 3000 to 12700 rpm to determine the optimal homogenizing time for the emulsion component. Fig. 4 demonstrates that raising the homogenizer speed from 3000 to 5800 rpm for a contract duration of 9 minutes results in an improvement in emulsion stability, removal, and stripping of efficiency, with the related increases being from 1.302% to 0.745%, from 89% to 96%, and from 85% to 92% respectively. The interior droplets shrank as rotation rates rose, leading to the above effects. By increasing the droplets' surface area in this way, the rate at which solutes are transported is accelerated. A high viscosity emulsion was formed when the homogenizing speed was set to 12700 rpm. As a result, bigger droplets of emulsion formed, which decreased the stability of the emulsion. This could be the result of small drops rapidly coalescing into larger droplets, it causes the emulsion volume to rise

and eventually break. Because of this, Since the emulsifier tends to be unstable and easily break apart, it is not necessary to homogenize the speed at a very high speed [24]. A higher speed of the homogenizer at 12700 rpm led to an increase in the breakage percentage of

1.23%, as well as a decrease in the extraction efficiency at 88% and the stripping efficiency at 83% respectively. It was found through the studies that the ideal speed for the homogenizer is 5800 rpm.

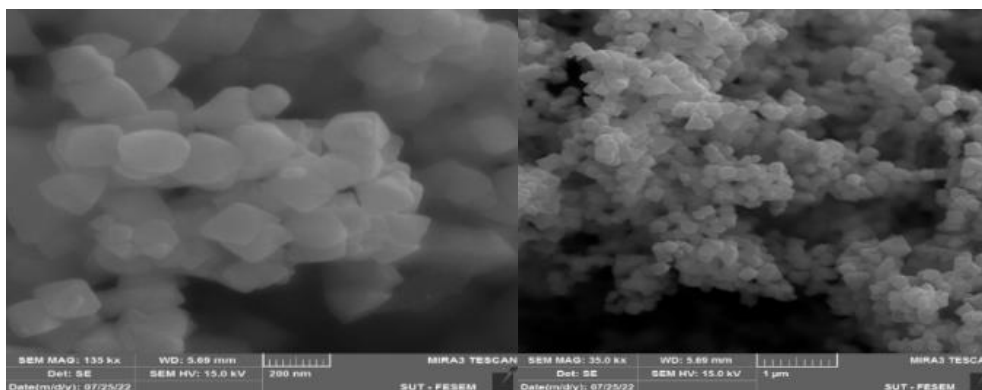


Fig. 3. SEM Image of Fe_3O_4 Nanoparticles

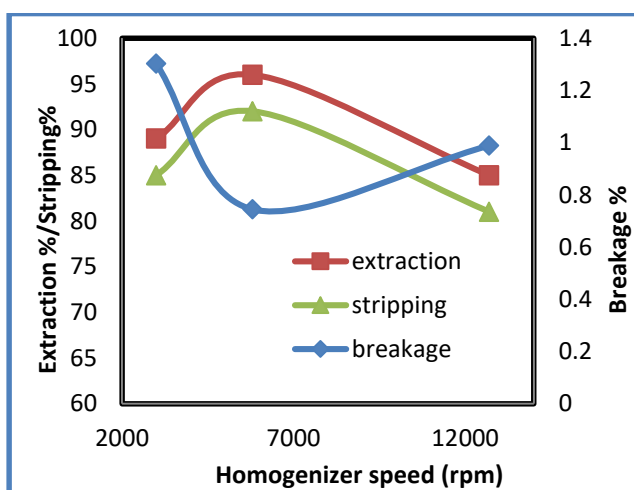


Fig. 4. Homogenizer Speed Effect on the Breakage, Stripping and Extraction of Membrane (Phenol Concentration =100ppm, External Phase pH=6.5, Span80 Concentration: 3% (v/v), ET: 5min., Stirrer Speed: 250 rpm, 0.1M NaOH, $\text{Fe}_3\text{O}_4=0.2\%$)

4.4. Span 80 Concentration

The ELM process is significantly impacted by the surfactant, which is a crucial parameter. A surfactant is an organic molecule that is polar has a tail that is hydrophobic and a hydrophilic head. As a result of the impossibility of diffusing the internal water phase within the oil membranes phase, when there is no surfactant present, an emulsion cannot be generated. When the concentration of the surfactant is below the optimal value, the membrane loses some of its stability, but a thick emulsion forms when the concentration is raised over that amount. Experiments were conducted with span 80 concentrations in the presence of 0.2% (w/v) nanoparticles of Fe_3O_4 with concentrations ranging from 1% to 7% (v/v), with all other parameters being the same, in order to explore the influence that this factor has on the stability of the emulsion and the efficacy of extraction. In

spite of the fact that it was assumed that the emulsion became more stable as the span 80 concentration increased, it was found that above a certain level of span 80 concentration, the stability remained essentially unchanged. This was due to the interface between the oil and the water had become saturated [25]. Fig. 5 shows that enhancing the span 80 concentration from 1% to 3% increases the extraction degree of phenol. Above this concentration of surfactant, a reduction in the extraction efficiency decreased again. This is due to the fact that excessive surfactant concentration tends to increase the viscosity of the membrane solution which leads to an increase in the resistance at the interface; hence the extraction degree of phenol was decreased [24]. As a result, the extraction concentration of 3% Span 80 was determined to be the most effective choice.

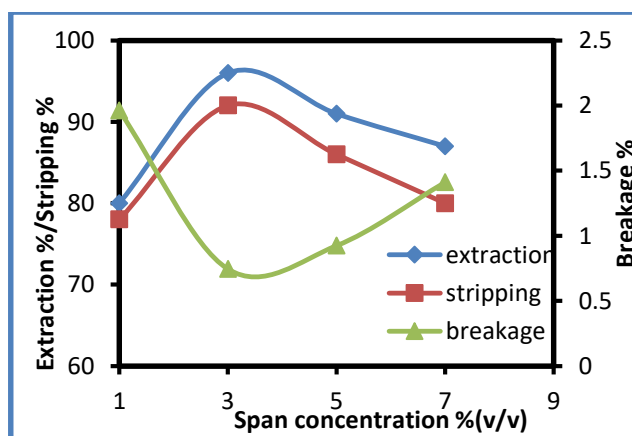


Fig. 5. Concentration Effect of Span80 on the Phenol Extraction with Time (External Phase pH=6.5 Homogenizer, Speed :5800 rpm, ET: 5min., Stirrer Speed: 300rpm, 0.1M NaOH, $\text{Fe}_3\text{O}_4=0.2\%$)

4.5. Fe_3O_4 Nanoparticles

The addition of Fe_3O_4 into the phase of membranes during PELM serves to enhance the stability of the

emulsion, which, in turn, reduces the amount of surfactant that is necessary for the process. In the work, Fe_3O_4 nanoparticles were added at concentrations ranging between 0.1% and 0.6% (w/v) in order to explore the impact these nanoparticles have on the efficacy of extraction and the emulsions of stability. The concentration of span 80 was held constant at 3% across all of the prior trials. The emulsion becomes more stable (the percentage of breakup decreases from 1.961% for 0.1% (w/v) Fe_3O_4 nanoparticles of 0.745% at 0.2% (w/v) correspondingly, shown as a Fig. 6. Due to the fact that this ratio covered a greater number of droplet interfaces [26]. However, on the other side, a breakage of larger occurred as the concentration of Fe_3O_4 nanoparticles was increased even further. The maximum efficiency of extraction, 96%, was attained at 0.2% (w/v), and it fell after that. This was because raising the emulsion stability through covering the emulsion contact caused the emulsion to become more stable, which caused the efficacy of extraction to decline. However, the extract efficiency dropped to nearly 80% when the concentration of Fe_3O_4 nanoparticles was increased beyond what was necessary to fully cover the emulsion droplets. This is due to the fact that the nanoparticles are capable of being distributed in a continuous phase, Furthermore, some of the particles could potentially generate new particles at the water/oil contact, increasing mass-transfer resistance during phenol transport. Similar trends were observed by [24, 26, 27]. Hence 0.2% (w/v) Fe_3O_4 nanoparticles were chosen in this work.

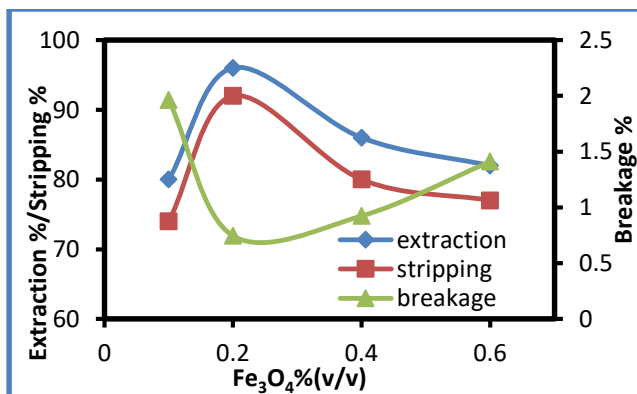


Fig. 6. Concentration Effect of Fe_3O_4 on the Phenol Extraction with Time (External Phase pH=6.5, Homogenizer Speed:5800 rpm, ET: 5min., Stirrer Speed: 300rpm, 0.1M NaOH, $\text{Fe}_3\text{O}_4=0.2\%$)

4.6. Mixing Speed

The impact of the mixing speed (rpm) of 200, 250, 300, and 350 rpm was tested on the process of removal of the phenol, as shown in Fig. 7, where the lowest percentage of breakage to 0.745% and the highest removal and stripping efficiency of phenol of 96% and 92% respectively, obtain at 300rpm and 5 min of emulsification time. The 300 rpm was found to be the desire for increasing the emulsion stability as it displays the lowest amount of emulsion leakage. Producing a greater shear force on the droplets significantly reduces

the emulsion globule's size, and increases the contact area [28]. When the mixing intensity is low, the emulsion globules get larger, which results in less surface area coming into touch with one other. Because high intensity causes globules to break, increasing the agitation speed in rpm can result in a decrease in the emulsion's stability [28].

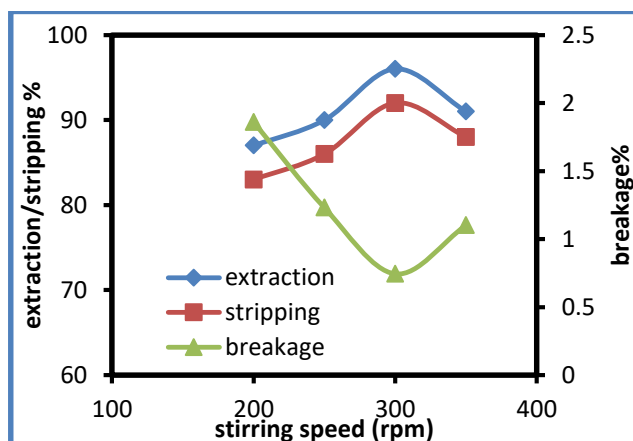


Fig. 7. Stirring Speed Effect on the Breakage, Stripping and Extraction of Membrane (Concentration of Phenol =100ppm, External Phase pH=6.5, Homogenizer Speed:5800 rpm, Span80:3%(v/v), ET: 5min., 0.1M NaOH, $\text{Fe}_3\text{O}_4=0.2\%$)

4.7. Effect of the Internal to Membrane Phase Volume Ratio

When there is a sufficient amount of the internal to membrane phase volume, the thickness of the phenol interface can be reduced, which in turn leads to an improvement in the transfer of the solutes over the course of the membrane phase. The ratio of the volume of the internal phase to the volume of the membrane phase during the experiment from 1:3 to 3:1 so that we may evaluate the influence that this difference has on the process of extraction of phenol and its ability to remain stable. Fig. 8 illustrates the profiles of the efficacy of extraction as well as the phenol breakage. The ratio was shifted between 1:3 to 1:1 by maintaining the same volume of membrane and interior phases, which resulted in a reduction in the amount of membrane breakdown from 2.395 to 0.745% and an increase in the amount of phenol extracted from around 85 to 96%. the 1:3 volume ratio is to blame for this peculiar pattern of behavior, an excessive amount of oil phase volume leads to the creation of increased emulsion thickness and viscosity, which stops the internal phase from spreading through the oil membrane. This drop in extraction efficiency is caused by the decreased availability of stripping agents, in order to reabsorb the solute through the membrane of phase. Because of an increase in membrane phase of volume in a bigger size of droplet as well as a higher membrane surface tension, it is difficult to disperse the water-in-oil emulsion droplets [29]. When the inner phase volume is triple that of the membrane phase, the volume ratio rises about 1:1 to 3:1. caused the emulsion's stability to

deteriorate in a way that was clearly (1.492% efficiency of breakage), and the removal effectiveness was reduced to somewhere around 88%. This drop is due to there not being enough volume in the membrane of phase, That the interior droplet cannot be completely ensnared is the implication of this. As a consequence of this, it has a propensity for migrating beyond the boundaries of the emulsion bubbles and into the exterior phase. Previous research also found that this volume-to-performance ratio was effective [30-32]. Therefore, the ratio of the volume of 1:1 between the internal phase and the membrane phase was chosen as the optimal ratio to produce a minimum of membrane breakage and the maximum possible phenol extraction efficiency.

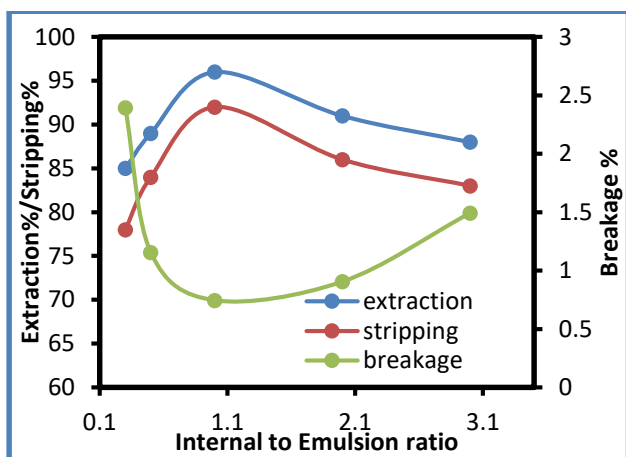


Fig. 8. Internal Effect on the Ratio of Emulsion Volume on the Breakage, Stripping, and Extraction of Membrane (Homogenizer Speed:5800 rpm, Span80: 3%(v/v), ET: 5min., Stirrer Speed: 300rpm, 0.1M NaOH, $Fe_3O_4=0.2\%$)

4.8. Effect of Emulsification Time

Fig. 9 shows the effect of emulsification time on Pickering emulsion stability, extraction, and stripping efficiencies. At 5 minutes of emulsification time, displayed the minimal breakage percent, which was 0.745%. in addition to the highest possible phenol removal and stripping efficiency, which were 96% and 92% respectively. When the emulsification duration was insufficient, which was 3 minutes, the breakage percentage of phenol was 1.32%, its extraction efficiency was 85%, and its stripping efficiency was 78%. occurred because the droplets are bigger, coalescence was made easier at the shorter emulsification time. [25] observed a higher breakage of the emulsion at the lower emulsification time. When compared to this, the extraction and stripping efficiencies dropped by 92% and 88%, respectively, when the emulsification period was more than 5 minutes, while the breakage percent increased to 0.953% with increasing the emulsification time from 5 to 7 min. This is because of the strong interior shearing, resulting in a significant increase in the number of very minute droplets per volume unit, which facilitates their diffusion into the exterior phase [24]. As a

result, the optimal emulsification time was determined to be 5 minutes throughout this investigation.

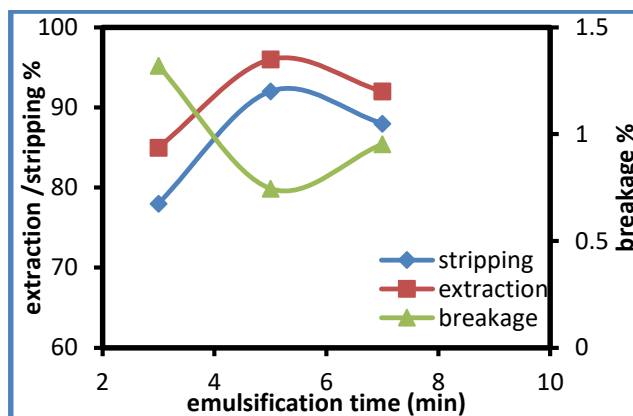


Fig. 9. Emulsification Time Effect on the Efficiency of Breakage, Stripping, and Extraction of Membrane (External Phase pH=6.5, Homogenizer Speed:5800 rpm, Span80 =3%(v/v)., Stirrer Speed: 250 rpm, 0.1M NaOH, $Fe_3O_4=0.2\%$)

4.9. Effect of External Phase pH

In the phenol extraction process, the pH of the exterior phase is significant. This may impact the phase membrane stability since pH values of high or low can accelerate the method of droplets separating from an emulsion. The findings of experiments conducted with acidic, neutral, and alkaline pH values between 4.5 and 8.5 are displayed in Fig. 10. In conditions of high acidity (pH = 4.5), The efficiency of the extraction was only approximately 84%, while the proportion of breakage reached its highest approximately 1.346%. That may be owing to greater concentrations of H^+ , which results in a decreased pH, which results in the phenol undergoing a process of destabilization. On the other hand, decreasing removal efficiency is likely related to the extractant with a neutral, which, at this pH range, is unable to form a compound with the molecules of phenol in a sufficient enough manner. At pH=6.5, however, phenol extraction efficiency was increased at 96%, while emulsion breakage was little influenced. Breakage also increased to 1.169% when the pH was 8.5, while the efficiency of extraction dropped to around 88%. It is possible that this phenomenon can be accounted for by the fact that protons are liberated as a result of the reaction exchange of anion reaction [33]. Additionally, different species form when pH rises. Keeping the pH of the external phase at 6.5 was ideal for continuing the study.

4.10. Effect of NaOH Concentration

Since the fact that the removal process takes place at the interface between the LM and the external phase of the solution, the extraction of species must inevitably involve a simultaneous stripping process on the other side of the membrane [34]. In this work, the examination was also done on the effect imposed by the concentration of NaOH on the degree of extraction in order to raise the phenol

concentration in the stripping phase and boost the regeneration of the membrane. When the concentration of NaOH was increased from 0.01 to 0.1 M, as shown in Fig. 11, the efficiency of phenol extraction and stripping increased, respectively, from 76% to 96% and from 70% to 92%. When the concentration of NaOH was increased above 0.1 M, the percentage of breakage decreased from 2.415 to 0.745%. However, the phenol extraction and stripping efficiency both decreased throughout this process. This could have occurred because an increase in the concentration of NaOH in the stripping phase brought about a reduction in the difference in densities and a buildup of the emulsion's viscosity, both of which were reflected in the increased droplet sizes. In addition, the emulsion stability decreased when the sodium hydroxide concentration was increased, which was a reaction caused by the interaction between the sodium hydroxide and the surfactant. A portion of its surfactant qualities were also lost as a consequence of this, which led to the destabilization of the emulsion and a reduction in the amount of material that could be extracted [35]. As a result, for the purposes of this investigation, the 0.1 M NaOH concentration was chosen since it led to a greater proportion of extraction and a lower degree of breakage.

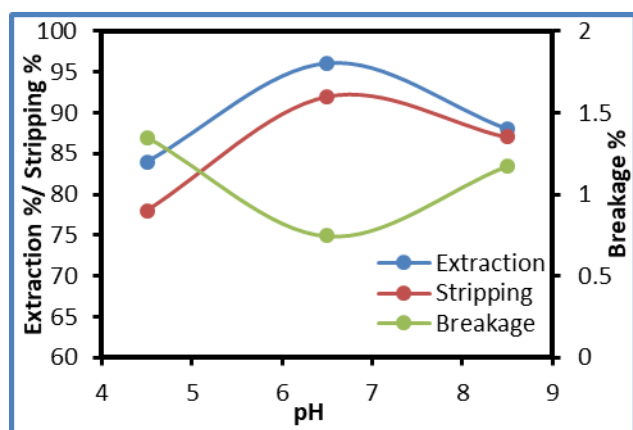


Fig. 10. Effect of External Phase pH on Removal Efficiency (Phenol Concentration =100ppm, Homogenizer Speed:5800 rpm, Concentration of Span80: 3% (v/v), ET: 5min., Stirrer Speed: 300rpm, 0.1M NaOH, Fe_3O_4 Concentration= 0.2%)

4.11. Effect of Phenol Concentrations

In the current work, the optimal parameter values for the extraction of phenols were studied using Pickering emulsion liquid membranes. These membranes were stabilized by both a surfactant and a solvent. Because of their inexpensive cost, non-harmful effects on the surrounding environment, and relative lack of toxicity, magnetic Fe_3O_4 nanoparticles were selected for use as stabilizers for Pickering emulsions [36]. In this study, the extraction processes for phenol were investigated at a variety of concentrations, including 25, 50, 75, 100, and 200 ppm. Fig. 12 displays the impact that the amount of phenol has on how efficiently the extraction process works. For the feed phase solution, the phenol extraction

efficiency was at its highest when the concentration was 100 mg/L; however, after the concentration was raised over 100 mg/L, the efficiency of phenol extraction began to drop. It is because of this region's interface between the external feed phase and the liquid membrane phase that the extraction efficiency of phenol is reduced. This region quickly becomes saturated with phenol ions. Due to the high phenol concentration, the phenol compounds diffuse across the membrane phase at an extremely sluggish rate. This is because of the increased mass transfer barrier that the higher phenol concentration creates [37]. When there was a concentration of phenol during the feed phase of 100 mg/L, a removal efficiency of phenol ion that was at its highest possible level of 96% was measured and recorded. when increasing the concentration of phenol above the critical value to 200 mg/L caused to reduction in extraction efficiencies to 94%. This behavior occurs because of the quick saturation of the internal droplets that leads to a longer diffusion path and lower yield of phenol removal [38]. A feed phenol concentration of 100 ppm was indicated as the optimal concentration.

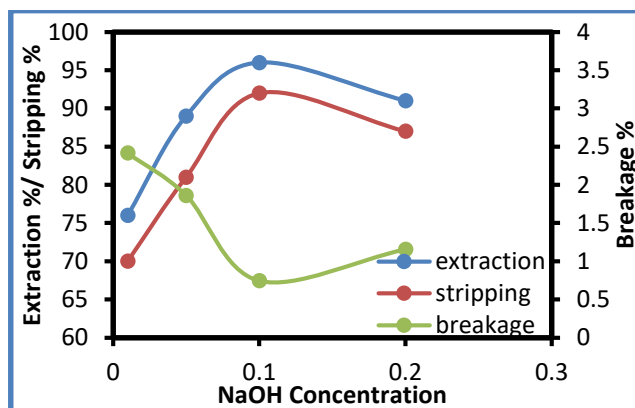


Fig. 11. NaOH Concentration Effect on the Breakage, Stripping and Extraction of Membrane (External Phase pH=6.5, Homogenizer Speed:5800 rpm, Concentration of Span80: 3% (v/v), ET: 5min., Stirrer Speed: 300rpm Fe_3O_4 Concentration= 0.2%)

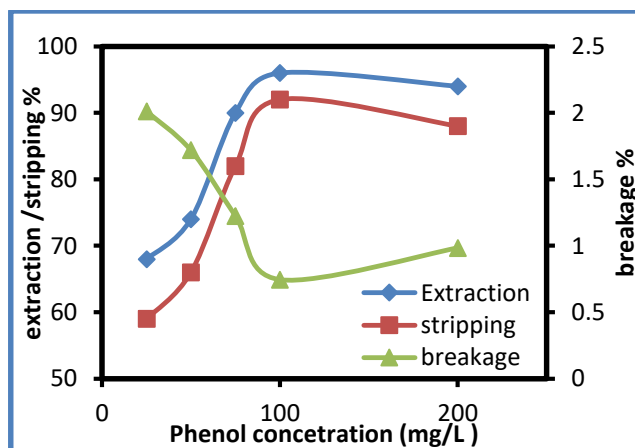


Fig. 12. Phenol Concentration Effect on the Breakage, Stripping and Extraction of Membrane (External Phase pH=6.5, Homogenizer Speed:5800 rpm, Concentration of Span80: 3% (v/v), ET: 5min., Stirrer Speed: 300rpm Fe_3O_4 Concentration= 0.2%)

4.12. Temperature Influence and Thermodynamic

Extraction efficiency and emulsion stability are both affected by temperature, making it a crucial parameter. The effects of a rise in extraction temperature are summed up in the following expression: (1) The exterior feed phase viscosity has decreased, the membrane phase, and the inner phase. (2) a quickening in the rate of the reaction that takes place between the internal reagent and the solution. (3) A reduction in both the tension at the interface and the resistance encountered by solutes as they flow through the membrane. (4) Reduced emulsion stability as a result of a rise in the rate of surfactant hydrolysis and reduction in the emulsion phase's viscosity. As a consequence, the viscosity of the emulsion of phase is a significant factor in determining the degree to which the emulsion remains stable during the removal time [39] The temperature at which the removal is performed must therefore be at an optimum level [40]. In accordance with [38], The temperature of the feed has a major impact on the stability of the membrane as well as the efficiency of the extraction. During this experiment, the temperature was increased from 298K to 313K while all other variables remained unchanged. According to the data that was collected, there was a correlation between an increase in temperature from 298 to 303K and a rise in the extraction efficiency of phenol with the stability of the membrane. The efficient transport of phenol is made possible by a reduction in the membrane's viscosity, which is caused by an increase in temperature. When the temperature rises above 303 degrees Celsius, the phenol extraction efficiency drops. It's possible that the stripping agent (NaOH) has leaked into the feed solution. As a result, the best temperature for optimum was determined to be 30 °C. Researchers looked at how temperature affected the amount of material removed [41] at temperatures of 25, 30, 35, and 40 degrees Celsius, as shown in Fig. 13. The results that were collected showed that temperature had a substantial influence on the emulsion's ability to remain stable. The temperature ranges of 30 degrees Celsius was used to generate a stable emulsion.

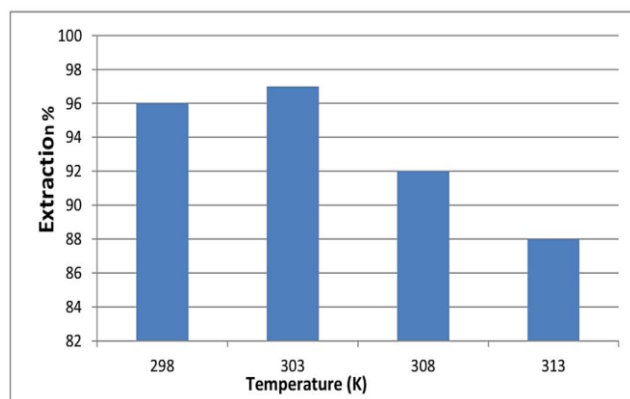


Fig. 13. Shows Temperatures and Extraction Efficiency

Thermodynamics studies were performed using the data obtained by the Van terhoff Eq. 4 to 7 [42].

Where: ΔH represents the enthalpy change (J/mol). ΔS represents the entropy change (J/mol). ΔG represents the Gibbs free energy change (J/mol. K).

$$K_c = \frac{C_o - C_e}{C_e} \quad (4)$$

$$\Delta G = -RT \ln K_c \quad (5)$$

$$\Delta G = \Delta H - T\Delta S \quad (6)$$

$$\ln(K_c) = \frac{\Delta S}{R} - \frac{\Delta H}{RT} \quad (7)$$

Where K_c : is the equilibrium constant. C_o and C_e : are the initial and equilibrium concentrations of phenol (mg/L). R : is the gas constant (8.314 J/mol.K). T : is the temperature (K).

Van't Hoff plots of ΔG against $1/T$ are drawn and ΔH , ΔS are obtained from the slope and intercept, respectively.

According to the data analysis in Table 2 and Fig. 14 for ELM. The value in the negative for ΔG indicates the potential for success of extracting phenol and the reaction is spontaneous. The value in the positive for ΔH shows that phenol extraction was an endothermic process. A value in the negative value for ΔS indicates that the extraction process was not random.

4.13. Recyclability

The nanoparticles of Fe_3O_4 and the phase of the membrane can be recycled and utilized in another extraction process, which of the following is a significant component of the PELM technique both as an economic and a Protection of the environment viewpoint. The nanoparticles, phase of oil, and extract are all components that have a low cost per unit, but their disposal into the environment can generate pollution that isn't desired. After the extraction procedure was finished, an apparatus known as a separating funnel was utilized in order to separate the emulsion from the transparent exterior phase. After that, the clear water solution from the outside was taken away, and the emulsion phase was demulsified by using a magnetic force from the outside to separate nanoparticles of Fe_3O_4 from the surface of the emulsion [26, 43]. After waiting for 60 minutes, the emulsion was allowed to break up into a phase of oil and an internal phase. After collecting particles of solid matter, they are cleaned through the use of water that has been distilled. following which it was dried at a temperature of 55 degrees Celsius for 10 hours. The membrane phase obtained was re-used under the optimal experimental conditions, which were as follows: the speed of homogenizer 5800 rpm, 5 minutes the emulsification time, 0.1 M NaOH internal phase, the ratio of internal to membranes ratio of 1 :1, 100mg/L for the phenol, pH 6.5, 300 rpm speed of mixing, and the ratio of external to the emulsion of 5/1. The phase of the membrane was obtained without the use of any additional extractant and Fe_3O_4 . The recyclability of the emulsion was effective all four times, and the efficacy of extraction was almost the same each time. However, after the fifth time through the

process, the efficiency of the extraction had begun to decline. This may be the result of the phase of the membrane and in particular, the material extracted becoming oversaturated with molecules of phenol as a result of continual recycling processes shown in Table 3, as well as the loss of extractant as a result of the partial

breakdown of extractant in phase of water [26]. Additionally, it was found the Fe₃O₄ used in the production of the phenol used in the removal of 4-Methoxyphenol and its separation may be recycled effectively three times.

Table 2. Thermodynamic Properties and their Values

Property	$\Delta H(\text{J/mol})$	$\Delta S(\text{J/mol})$	R^2	$\Delta G(\text{J/mol.K})$			
				298K	303K	308K	313K
Value	18.191	-52.472	0.6999	-7.873	-8.756	-6.253	-5.438

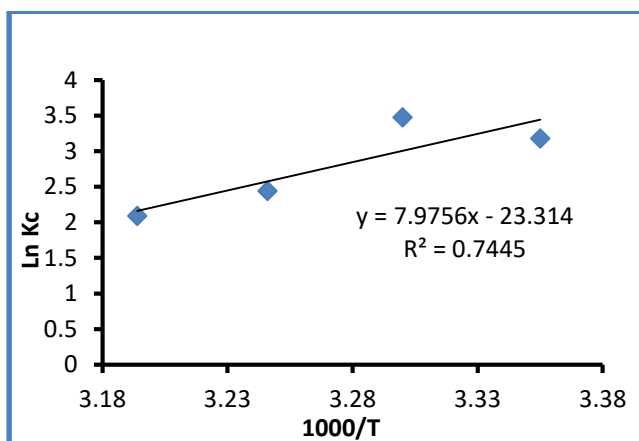


Fig. 14. Influence of Temperature on Phenol Extraction at Optimum Condition

Table 3. Show that the Membrane Phase and Fe₃O₄ Nanoparticles can be Recycled Five Times

Process	%Extraction efficiency	%Breakage percentage
Fresh	96.491	0.743
First recycle	95.942	0.974
Second recycle	95.049	1.183
Third recycle	93.172	1.416
Four recycle	91.995	1.602
Five recycle	88.730	2.518

5- Kinetic Study of Phenol Extraction by PELM

For determining the rate coefficients and application for each data, data were obtained from phenol extraction using the PELM method under optimal conditions. The kinetic investigation was conducted using the following equations [44].

We know,

- The equation for the zero-order rate is as follows:

$$A_{ct} = A_{ci} - Kt \tag{8}$$

- The equation for the first-order rate is as follows:

$$\ln A_{ct} = \ln A_{ci} - Kt \tag{9}$$

-The equation for the second-order rate is as follows:

$$\frac{1}{A_{ct}} = \frac{1}{A_{ci}} - Kt \tag{10}$$

Where: C_t : phenol of concentration present at the time (ppm). C_0 : concentration of phenol at the initial (ppm). t : period (mins).

At a temperature of 25°C, Fig. 15 a-c shows the results of the kinetic analysis utilizing the zero, first, and second reaction models. In Table 4, the evaluated constants and R^2 values are listed. Phenol extraction was found to come after a second-order reaction.

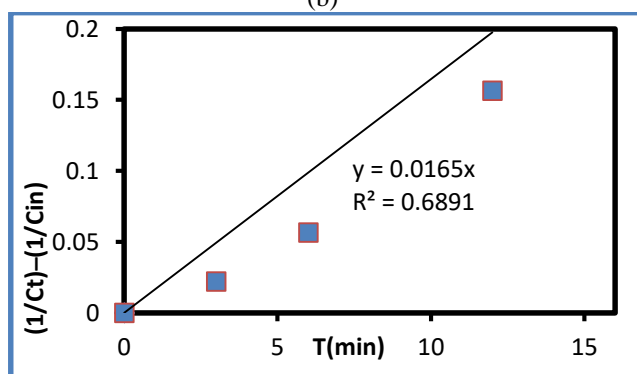
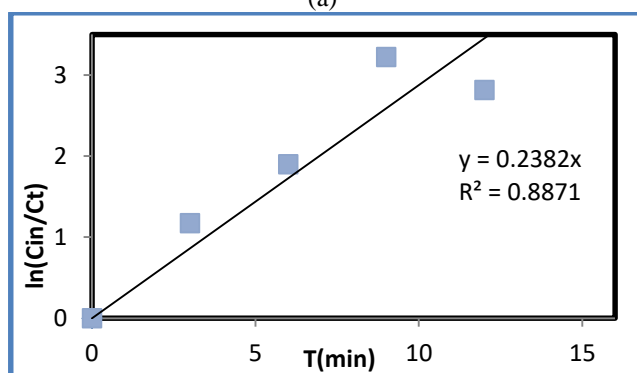
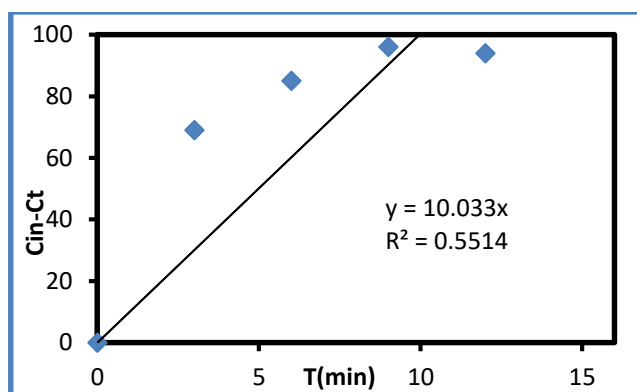


Fig. 15. (a) Zero Order, (b) First Order, (c) Second Order

Table 4. Kinetic Analysis Data

Order of reaction	Rate Constant value	R ² value
zero	10.033	0.5514
first	0.2382	0.8871
second	0.0165	0.6891

The extraction rate constant (K_{obs}) is represented by the slope of the straight lines. Additionally, it demonstrates that first-order kinetics was used for phenol extraction. When PELM was used, the phenol extraction rates were obtained as 0.2875 min^{-1} . These findings suggest that using PELM speeds up phenol extraction. For the PELM system, Eq. 11 indicates the total coefficient of the mass transfer [45].

$$\frac{1}{K_o} = \frac{1}{K_M} + \frac{1}{K_F} \quad (11)$$

Where: K_o : indicates the total coefficient of the mass transfer for PELM (m/s). K_M : The values of the phase of external coefficient for transfer of mass (m/s) Skell and Lee: correlations (m/s) that are provided by Eq. 12 below were utilized in order to estimate [46].

$$\frac{K_M}{\sqrt{ND}} = 2.932 * 10^{-7} \left(\frac{V_i + V_m}{V_i + V_m + V_e} \right) \left(\frac{d_i}{T} \right)^{0.548} Re^{1.371} \quad (12)$$

Where: N: the rate at which the feed phase is speed mixed (rpm). d_i : diameter of impeller (m). T: diameter of mixing tank (m). V_i, V_m, V_e : is defined as the volumes for space occupied through the phase of internal, phase of membrane, and the phases of external, in that order (mL). Re: represents the number of Reynold of the phase that is continuous and was computed based on the Eq. 13:

$$Re = \frac{Nd_i^2 \rho_c}{\mu_c} \quad (13)$$

Where: ρ_c : the density (kg/m³) for the phase of continuous. μ_c : the phase of continuous viscosity expressed in kilograms per meter per second.

The calculated value of Re was (264269.66). Whereas, D is the calculated membrane solute diffusivity (using the Wilke and Chang correlation) [47], showed in Eq. 14, which is found equal to $1.105 \times 10^{-11} \text{ m}^2/\text{s}$ for PELM.

$$D = \frac{117.3 \times 10^{-18} * (M \varphi)^{0.5} T}{\mu_m \varphi_c^{0.6}} \quad (14)$$

Where: M_φ is the typical diluent with a molecular weight of kerosene (170 kg/mol). T: temperature (k). φ : Diluent has an association factor of $\varphi_c = 1$. μ_m : The organic phase viscosity is ($176.05 \times 10^{-3} \text{ kg/m.s}$). φ_c : It is the phenol molar volume ($0.089 \text{ m}^3/\text{Kmol}$).

Which we determine with the use of the Schroeder formula. The constant of the interfacial rate of reaction, K_F (m/s) was determined utilizing an Eq. 15.

$$\ln\left(\frac{C_e}{C_{eo}}\right) = -A K_F t \quad (15)$$

On comparing Eq. 15 with Eq. 9, K_F can be identified through Eq. 16 below.

$$K_F = \frac{K_{obs}}{A} \quad (16)$$

Where: A: The emulsion's particular surface area at its interface with water is calculated by Eq. 17 [48].

$$A = \frac{A_i}{V} = \frac{6\alpha}{d_{32}} \quad (17)$$

Where: A_i : is the surface area of a droplet of emulsion(m²). V: It describes the volume of the emulsion in units. A: volume fraction of water = 1.

Table 5 displays the obtained mass transfer coefficients.

Table 5. Mass Transfer Coefficients of Phenol in the PELM Systems

Mass transfer coefficient (m/s)	PELM
K_M	4.0015×10^{-5}
K_F	11.16×10^{-7}
K_o	1.1159×10^{-6}

6- Conclusions

The current study investigates the application of Fe₃O₄ nanoparticles as a stabilizing factor in PELM for phenol extraction from an aqueous solution. PELM has proven to be a highly effective method for extracting phenol and is more stable than other methods. It is also simple to demulsify by using an external magnetic field to remove magnetic Fe₃O₄ from the emulsion. The ideal working conditions resulted in a maximum extraction percentage of 96% and a minimum breakage percentage of 0.745% at 9 minutes of contact time: 0.1 M NaOH in the internal phase, an emulsification speed of 5800 rpm, and 0.2% (w/v) Fe₃O₄ nanoparticles were used. Another Pickering emulsion was successfully created using the magnetic nanoparticles and membrane phase, and it extracted phenol for four cycles with almost the same extraction percentage. With an R²high value of 0.2875, kinetics analysis tests revealed that the first-order model was appropriate for phenol extraction. According to the thermodynamic analysis, the extraction process was endothermic. The overall mass transfer coefficient was obtained at PELM (when using kerosene, Fe₃O₄, and span 80), the mass transfer coefficient was $1.115 \times 10^{-6} \text{ m/s}$.

References

- [1] K. Wang Lawrence, Yung-Tse Hung, H. Lo. Lo Howard, Constantine Yapijakis, Handbook of Industrial and Hazardous Wastes Treatment, 2nd edition, MARCEL DEKKER, INC, 2004. <https://doi.org/10.1201/9780203026519>
- [2] V. Meda, T. Lope, R. Tyler, O.D. Baik, J. Soltan, Treatment of Phenol in Water Using Microwave-Assisted Advanced, 2014.
- [3] N. N. Li, Separating hydrocarbons with liquid membranes, U.S. Patent, 1968.
- [4] S. Bajpai, M. Bhowmik, Poly (acrylamide-co-itaconic acid) as a potential ion-exchange sorbent for effective removal of antibiotic drug-ciprofloxacin from aqueous solution, *Journal of Macromolecular Science, Part A*, 48 2010, 108-118. <http://dx.doi.org/10.1080/10601325.2011.534718>

- [5] B. De Witte, J. Dewulf, K. Demeestere, H. Van Langenhove, Ozonation and advanced oxidation by the peroxone process of ciprofloxacin in water, *Journal of Hazardous Materials*, 161 2009, 701-708. <https://doi.org/10.1016/j.jhazmat.2008.04.021>
- [6] S. Wu, Y. Li, X. Zhao, Q. Du, Z. Wang, Y. Xia, L. Xia, Biosorption behavior of ciprofloxacin onto *Enteromorpha prolifera*: isotherm and kinetic studies, *International journal of phytoremediation*, 17 2015, 957-961. <https://doi.org/10.1080/15226514.2014.935288>
- [7] V. Homem, L. Santos, Degradation and removal methods of antibiotics from aqueous matrices—a review, *Journal of environmental management*, 92 2011, 2304-2347. <https://doi.org/10.1016/j.jenvman.2011.05.023>
- [8] J. Fei, J. Zhao, H. Zhang, A. Wang, C. Qin, P. Cai, X. Feng, J. Li, One-pot mass selfassembly of MnO₂ sponge-like hierarchical nanostructures through a limited hydrothermal reaction and their environmental applications, *Journal of colloid and interface science*, 490 2017, 621-627. <http://dx.doi.org/10.1016/j.jcis.2015.07.076>
- [9] V.S. Antonin, M.C. Santos, S. Garcia-Segura, E. Brillas, Electrochemical incineration of the antibiotic ciprofloxacin in sulfate medium and synthetic urine matrix, *Water research*, 83 2015, 31-41. <http://dx.doi.org/10.1016/j.watres.2015.05.066>
- [10] Y. Wang, C. Shen, M. Zhang, B.-T. Zhang, Y.-G. Yu, The electrochemical degradation of ciprofloxacin using a SnO₂-Sb/Ti anode: influencing factors, reaction pathways and energy demand, *Chemical Engineering Journal*, 296 2016, 79-89. <https://doi.org/10.1016/j.cej.2016.03.093>
- [11] S. Melle, M. Lask, G.G. Fuller, Pickering emulsions with controllable stability, *Langmuir*, 21 2005, 2158-2162. <https://doi.org/10.1021/la047691n>
- [12] T. Liu, Kaiser, W. Richtering, A.M. Schmidt, Magnetic capsules and Pickering emulsions stabilized by core-shell particles, *Langmuir*, 25 2009, 7335-7341. <https://doi.org/10.1021/la900401f>
- [13] H. Liu, C. Wang, Q. Gao, X. Liu, Z. Tong, Magnetic hydrogels with supracolloidal structures prepared by suspension polymerization stabilized by Fe₂O₃ nanoparticles, *Acta biomaterialia*, 6 2010, 275-281. <https://doi.org/10.1016/j.actbio.2009.06.018>
- [14] X.-M. Liu, S.-Y. Fu, H.-M. Xiao, C.-J. Huang, Preparation and characterization of shuttle-like α -Fe₂O₃ nanoparticles by supermolecular template, *Journal of Solid State Chemistry*, 178 2005, 2798-2803. <https://doi.org/10.1016/j.jssc.2005.06.018>
- [15] B. Balaraju, M. Kuppan, S.H. Babu, S. Kaleemulla, M.M. Rao, C. Krishnamoorthi, G.M. Joshi, G.V. Rao, K. Subbaravamma, I. Omkaram, Structural, Optical and Magnetic Properties of α -Fe₂O₃ Nanoparticles, *Mechanics, Materials Science Engineering Journal*, 9, 2017.
- [16] M. Farahmandjou, F. Soflaee, Synthesis and characterization of α -Fe₂O₃ nanoparticles by simple co-precipitation method, *Physical Chemistry Research*, 3, 2015, 191-196. <https://doi.org/10.22036/pcr.2015.9193>
- [17] G.S. Demirer, A.C. Okur, S. Kizilel, Synthesis and design of biologically inspired biocompatible iron oxide nanoparticles for biomedical applications, *Journal of Materials Chemistry B*, 3 2015, 7831-7849. <https://doi.org/10.1039/C5TB00931F>
- [18] S.U. Pickering, Cxvii. —emulsions, *Journal of the Chemical Society, Transactions*, 91, 1907, 2001-2021. <http://dx.doi.org/10.1039/CT9079102001>
- [19] S. Behrens, San-Miguel, Influence of nanoscale particle roughness on the stability of pickering emulsions, *Langmuir*, 28 2012, 12038-12043. <https://doi.org/10.1021/la302224v>
- [20] L. Zhao, D. Fei, Y. Dang, X. Zhou, J. Xiao, Studies on the extraction of chromium(III) by emulsion liquid membrane, *Journal of Hazardous Materials*, 178 2010, 130-135. <https://doi.org/10.1016/j.jhazmat.2010.01.052>
- [21] S. Nosrati, N. Jayakumar, M. Hashim, Extraction performance of chromium (VI) with emulsion liquid membrane by Cyanex 923 as carrier using response surface methodology, *Desalination*, 266 2011, 286-290. <https://doi.org/10.1016/j.desal.2010.08.023>
- [22] T. Hyeon, Lee, S.S. Park, J. Chung, Y. Na, H.B., Synthesis of Highly Crystalline and Monodisperse Maghemite Nanocrystallites without a Size- Selection Process. *J. Am. Chem. Soc.*, 123, 51 2001, pp.12798-12801. <https://doi.org/10.1021/ja016812s>
- [23] R. Y. Hong, T. T. Pan, Y. P. Han, H. Z. Li, J. Ding and S. Han Magnetic field synthesis of Fe₃O₄ nanoparticles used as a precursor of ferrofluids. *Journal of Magnetism and Magnetic Materials*, 310, 1 2007, pp. 37-47. <https://doi.org/10.1016/j.jmmm.2006.07.026>
- [24] A. A. Mohammed and N. Q. Jaber, Stability and performance studies of emulsion liquid membrane on pesticides removal using mixture of Fe₃O₄ nanoparticles and span80. *Environmental Advances*, 9 2022, 100294. <https://doi.org/10.1016/j.envadv.2022.100294>
- [25] M. Gasser, N. El-Hefny, J. Daoud, Extraction of Co (II) from aqueous solution using emulsion liquid membrane. *Journal of Hazardous Materials*, 151, 2008, 610-615. <https://doi.org/10.1016/j.jhazmat.2007.06.032>
- [26] Z. Lin, Z. Zhang, Y. Li and Y. Deng, "Magnetic nano-Fe₃O₄ stabilized Pickering emulsion liquid membrane for selective extraction and separation." *Chemical Engineering Journal*, 288: 2016, 305-311. <https://doi.org/10.1016/j.cej.2015.11.109>

- [27] H. M. Salman, and A. A. Mohammed, Extraction of lead ions from aqueous solution by co-stabilization mechanisms of magnetic Fe₂O₃ particles and nonionic surfactants in emulsion liquid membrane. *Colloids and Surfaces A: Physicochemical and Engineering Aspects*, 568: 2019, 301-310. <https://doi.org/10.1016/j.colsurfa.2019.02.018>
- [28] Q. Al-Obaidi, M. Alabdulmuhsin, A. Tolstik, J. G. Trautman and M. Al-Dahhan. Removal of hydrocarbons of 4-nitrophenol by emulsion liquid membrane (ELM) using magnetic Fe₂O₃ nanoparticles and ionic liquid. *Journal of Water Process Engineering*, 39, 2021, 101729. <https://doi.org/10.1016/j.jwpe.2020.101729>
- [29] A. Ahmad, C. Kusumastuti, B. Derek, Ooi, Emulsion liquid membrane for cadmium removal: Studies on emulsion diameter and stability, *Desalination*, 287 2012, 30-34. <https://doi.org/10.1016/j.desal.2011.11.002>
- [30] N. Jusoh, N. Othman, N.A. Nasruddin, Emulsion liquid membrane technology in organic acid purification, *Malaysian Journal of Analytical Sciences*, 20 2016, 436-443. <http://dx.doi.org/10.17576/mjas-2016-2002-28>
- [31] A.A. Mohammed, H.M. Selman, Liquid surfactant membrane for lead separation from aqueous solution: Studies on emulsion stability and extraction efficiency, *Journal of Environmental Chemical Engineering*, 6 2018, 6923-6930. <https://doi.org/10.1016/j.jece.2018.10.021>
- [32] S. Zereshki, P. Daraei, A. Shokri, Application of edible paraffin oil for cationic dye removal from water using emulsion liquid membrane, *Journal of Hazardous Materials*, 356 2018, 1-8. <http://dx.doi.org/10.1016/j.jhazmat.2018.05.037>
- [33] M. A. Hussein, A. A. Mohammed, M. A. Atiya. Application of emulsion and Pickering emulsion liquid membrane technique for wastewater treatment: an overview. *Environmental Science and Pollution Research*, Vol. 26, Issue 36, 2019, 36184–36204. <https://doi.org/10.1007/s11356-019-06652-3>
- [34] R.A. Kumbasar. Selective separation of chromium (VI) from acidic solutions containing various metal ions through emulsion liquid membrane using trioctylamine as extractant. *Separation purification technology*, 64(1), 2008, 56–62. <https://doi.org/10.1016/j.seppur.2008.08.005>
- [35] A. A. Mohammed and R. W. Al-Khateeb. Application of Emulsion Liquid Membrane Using Green Surfactant for Removing Phenol from Aqueous Solution: Extraction, Stability and Breakage Studies. *Journal of Ecological Engineering*, 2022, 23, 1. <http://dx.doi.org/10.12911/22998993/143970>
- [36] F. H. Al-Ani, Q. F. Alsalhy, and M. Al-Dahhan. Enhancing emulsion liquid membrane system (ELM) stability and performance for the extraction of phenol from wastewater using various nanoparticles. *Desalination and Water Treatment*, 210, 2021, 180-191. <https://doi.org/10.5004/dwt.2021.26547>
- [37] N. Rajamohan, M. Rajasimman, F. Al Qasmi, Parametric studies on the removal of nickel using emulsion liquid membrane, *Desalination and Water Treatment*, 141 2019, 89–94. <http://dx.doi.org/10.5004/dwt.2019.23426>
- [38] S. Sujatha, N. Rajamohan, Y. Vasseghian, M. Rajasimman, Conversion of waste cooking oil into value-added emulsion liquid membrane for enhanced extraction of lead: Performance evaluation and optimization, *Chemosphere*, 284 2021, 131385. <https://doi.org/10.1016/j.chemosphere.2021.131385>
- [39] P.F.M.M. Correia, J.M.R. de Carvalho, Recovery of phenol from phenolic resin plant effluents by emulsion liquid membranes, *Journal of Membrane Science*, 225 2003, 41–49. [https://doi.org/10.1016/S0376-7388\(03\)00319-3](https://doi.org/10.1016/S0376-7388(03)00319-3)
- [40] K. Abbassian, A. Kargari, Effect of polymer addition to membrane phase to improve the stability of emulsion liquid membrane for phenol pertraction, *Desalination and Water Treatment*, 57 7 2016, 2942–2951. <https://doi.org/10.1080/19443994.2014.983981>
- [41] H. K. Admawi and A. A. Mohammed. A comprehensive review of emulsion liquid membrane for toxic contaminants removal: An overview on emulsion stability and extraction efficiency. *Journal of Environmental Chemical Engineering*, 2023, 109936. <https://doi.org/10.1016/j.jece.2023.109936>
- [42] W. Long, C. Yang, G. Wang and J. Hu. Effective adsorption of Hg (II) ions by new ethylene imine polymer/ β -cyclodextrin crosslinked functionalized magnetic composite. *Arabian Journal of Chemistry*, 16 2 2023, 104439. <https://doi.org/10.1016/j.arabjc.2022.104439>
- [43] J. Liang, H. Li, J. Yan, W. Hou, Demulsification of oleic-acid-coated magnetite nanoparticles for cyclohexane-in-water nanoemulsions, *Energy Fuels*, 28 2014 6172-6178. <https://doi.org/10.1021/ef501169m>
- [44] D. Sharmmah and J. Manuel. Extraction of methylene blue from aqueous solution by pickering emulsion liquid membrane using cellulose as eco-friendly emulsifier: optimization and modeling studies. *Water Science and Technology*, 871 2023, 174-192. <https://doi.org/10.2166/wst.2022.405>

- [45] H. Kasaini, F. Nakashio, M. Goto. Application of emulsion liquid membranes to recover cobalt ions from a dual-component sulphate solution containing nickel ions. *Journal of Membrane Science*, 1462 1998, 159–168.
[https://doi.org/10.1016/S0376-7388\(98\)00105-7](https://doi.org/10.1016/S0376-7388(98)00105-7)
- [46] M. Raji, H. Abolghasemi, J. Safdari, A. Kargari, Selective extraction of dysprosium from acidic solutions containing dysprosium and neodymium through emulsion liquid membrane by Cyanex 572 as carrier, *Journal of Molecular Liquids*, 254, 2018, 108-119.
<https://doi.org/10.1016/j.molliq.2017.11.058>
- [47] R.E. Treybal. Mass – Transfer Operations, third ed., McGraw-Hill Book Co, Singapore, 1981.
- [48] V. Karcher, F. Perrechil, A. Bannwart. Interfacial energy during the emulsification of water-in-heavy crude oil emulsions. *Brazilian Journal of Chemical Engineering*. 32 2015, 127–137.
<https://doi.org/10.1590/0104-6632.20150321s00002696>

إزالة ملوثات الفينول من محلول مائي باستخدام غشاء سائل مستحلب بيكرينغ المثبت بواسطة مغناطيسي نانو Fe_3O_4

تمارا لؤي رسول^{١*}، أحمد عبد محمد^١، ويدا روان خواه^٢

^١ قسم الهندسة البيئية، كلية الهندسة، جامعة بغداد، بغداد، العراق

^٢ قسم الهندسة الكيميائية، جامعة كرمانشاه التكنولوجية، كرمانشاه، إيران

الخلاصة

في الدراسة الحالية، تم فحص تأثير الفاعل بالسطح غير الأيوني الممتد ٨٠ على استحلاب خليط من الكيروسين كمذيب عضوي قائم على البترول وامتداد ٨٠ كمخفف أخضر بنسبة ١:١. تم استخدام هيدروكسيد الصوديوم كمرحلة داخلية، وتم اختبار ثبات المستحلب. تم استكشاف إمكانية استخلاص الفينول من المحاليل المائية دون استخدام عامل ناقل باستخدام غشاء سائل مستحلب بيكرينغ. بالإضافة إلى ذلك، تشمل تأثيرات المعلمات التجريبية سرعة المجانس، وسرعة الخلط، ووقت الاستحلاب، ونسب Fe_3O_4 , Span 80، وتركيز هيدروكسيد الصوديوم، ونسبة حجم الغشاء الداخلي إلى (I / O) على فعالية الاستخراج واستقرار المستحلب. أظهرت النتائج أنه بعد ٩ دقائق من وقت الاتصال ونسبة كسر بحد أدنى ٠,٧٤٥٪ في ظل الظروف المثالية، يمكن استرداد أكثر من ٩٦٪ من الفينول. بالإضافة إلى ذلك، يكشف التحليل الديناميكي الحراري أن عملية الاستخراج كانت ماصة للحرارة وعفوية بطبيعتها وأن معامل نقل الكتلة الكلي كان $(1.115 \times 10^{-6} m/s)$. تم إعادة تدوير المواد الغشائية والجسيمات النانوية أربع مرات في استخلاص الفينول بنفس الكفاءة تقريباً وبدون نسبة كسر ملحوظة.

الكلمات الدالة: غشاء سائل مستحلب بيكرينغ، تجريد، كفاءة، استخلاص، استقرار المستحلب، الكسر.